mate. The individual phases can then be determined from the twofold estimated invariants, provided that there exists a redundant set of accurately estimated invariants.

5. Concluding remarks

The presently available theory for the estimation of the three-phase structure invariants, *via* combined direct methods - anomalous dispersion techniques, has been reexamined. The analysis shows that these techniques do not yield one or two but rather eight possible estimates of the invariants. This, naturally, appears at first to limit severely the applicability of these techniques. Preliminary test calculations indicate, however, that in many cases the eight possible estimates are clustered around one or two values. Distinguishing these cases from those in which the eight estimates are widely scattered results in a significant gain in accuracy. Extensive calculations, based on the strategy described in § 4, are now in progress. Their results will be presented in the near future.

Details of the test calculations

All of the calculations were done using calculated diffraction data for the $PtCl_4^{2-}$ derivative of cytochrome c_{550} (Timkovich & Dickerson, 1973, 1976). The coordinates were obtained from the Protein Data Bank (Bernstein *et al.*, 1977). The calculations were done on a 16-bit PDP11/23 computer. The programs used were written by S. A. Potter and C. M. Weeks of the Medical Foundation of Buffalo, Inc., and adapted by Nancy J. Moore.

We thank S. A. Potter and C. M. Weeks for making their computer programs available to us, and R. H. Blessing for his critical reading of the manuscript. Financial assistance from the Natural Sciences and Engineering Research Council of Canada and from Queen's University is gratefully acknowledged.

References

BERNSTEIN, F. C., KOETZLE, T. F., WILLIAMS, G. J. B., MEYER, E. P. JR, BRICE, M. D., RODGERS, J. R., KENNARD, O., SHIMANOUCHI, T. & TASUMI, M. (1977). *J. Mol. Biol.* **112**, 535-542.

FORTIER, S., MOORE, N. J. & FRASER, M. E. (1985). *Acta Cryst.* A**41**, 571-577.

GIACOVAZZO, C. (1983). *Acta Cryst.* A**39**, 585-592.

HAUPTMAN, H. (1972). *Crystal Structure Determination: The Role of the Cosine Seminvariants.* New York and London: Plenum Press.

HAUPTMAN, H. (1982). *Acta Cryst.* A**38**, 632-641.

KROON, J., SPEK, A. L. & KRABBENDAM, H. (1977). *Acta Cryst.* A**33**, 382-385.

OKAYA, Y. & PEPINSKY, R. (1956). *Phys. Rev.* **103**, 1645-1647.

PEEDERMAN, A. F. & BIJVOET, J. M. (1956). *Proc. K. Ned. Akad. Wet.* B**59**, 312-313.

PONTENAGEL, W. M. G. F. (1983). Thesis, Univ. of Utrecht.

RAMACHANDRAN, G. N. (1964). Editor. *Advanced Methods of Crystallography.* London and New York: Academic Press.

RAMACHANDRAN, G. N. & RAMAN, S. (1956). *Curr. Sci.* **25**, 348-351.

RAMASESHAN, S. & ABRAHAMS, S. C. (1975). Editors. *Anomalous Scattering.* Copenhagen: Munksgaard.

SAYRE, D. (1982). Editor. *Computational Crystallography.* Oxford: Clarendon Press.

TIMKOVICH, R. & DICKERSON, R. E. (1973). *J. Mol. Biol.* **79**, 39-56.

TIMKOVICH, R. & DICKERSON, R. E. (1976). *J. Biol. Chem.* **251**, 4033-4046.

Acta Cryst. (1986). A**42**, 156-164

Single-Crystal Structure of Rapidly Cooled Alloys with Icosahedral Symmetry. I. Experimental Analysis

BY GABRIELLE G. LONG AND MASAO KURIYAMA

Institute for Materials Science and Engineering, National Bureau of Standards, Gaithersburg, MD 20899, *USA*

(*Received* 27 *March* 1985; *accepted* 4 *November* 1985)

Abstract

Crystallographic analysis is applied to a set of electron diffraction patterns taken from a rapidly cooled Al-Mn alloy to construct reciprocal-lattice patterns in agreement with the observed icosahedral results. The analysis leads to a proposed atomic scale model which is derived from two sets of experimental modulations, each of which has six independent modulation vectors. The underlying structure has a lattice, the unit cell of which involves 32 atomic sites with the required symmetry properties. The appearance of the experimental electron diffraction patterns is explained either by the coherent arrangement of this

lattice with an irrational sublattice or by an independent set of modulations. The relationship of this structure to three-dimensional nonperiodic Penrose tilings is explored.

1. Introduction

Since the early part of this century, when Laue (1912) proposed that the observed diffraction pattern of X-rays by a crystal was due to the interaction between the wave nature of light and the periodicity of the arrangement of atoms in a crystal, it has been thought that long-range translational invariance (which defines a crystal) is required to produce sharp diffraction peaks. The crystal lattice has historically been described in terms of its translation, reflection, rotation and inversion symmetries. While a molecule can have any symmetry, an infinite-periodic lattice cannot have, for example, $2\pi/5$ or $2\pi/7$ rotational symmetry (Kittel, 1976) because the five- or sevenfold axis cannot be used to fill all of space periodically. Recently, Mackay (1981, 1982) suggested a new crystallography in which fivefold patterns may be observed. The mechanism by which he creates the conditions for observing this previously disallowed symmetry is to fill space nonperiodically with more than one primitive cell. The simplest case involves two rhombohedra which are fitted together according to a nonperiodic three-dimensional Penrose (1974) tiling. The rules for filling space are based on the Fibonacci sequence (Hoggatt, 1969) involving the lengths one and τ, where τ is equal to $(1+\sqrt{5})/2$, and is known as the Golden Section. Kramer & Neri (1984) have demonstrated the association between the icosahedral group $A(5)$ and the three-dimensional generalization of the Penrose tiling *via* the two rhombohedra.

While it may not be surprising that three-dimensional space can be filled nonperiodically by two or more primitive cells, it is surprising at first to find that there can exist perfect long-range correlations in such a structure. The recent discovery of a metallic 'icosahedral phase' by Shechtman, Blech, Gratias & Cahn (1984) has added further impetus to this work.

In that experiment on rapidly cooled Al-14 at. % Mn, a set of electron diffraction patterns were acquired which suggest orientational order and icosahedral point-group symmetry. Levine & Steinhardt (1984) then proposed a 'quasicrystal' model (which is nonperiodic as outlined above) to explain the three- and fivefold diffraction patterns.

What has not yet been demonstrated is how the nonperiodic structures relate to the underlying atomic order of the material, and what is the explicit connection to the sharp delta-function-like diffraction patterns obtained. In particular, should the structure be described as nonperiodic but ordered or as an incommensurate modulated crystal that may require a generalization of our current understanding of modulations?

The new phase is fabricated by rapid cooling of molten aluminium-14-20 at. % manganese using melt spinning. The result is a rather brittle ribbon ~2 mm wide and ~40 μm thick. The object of interest is a flower-shaped crystal approximately 2 μm in diameter. In so far as we know, single-phase binary alloy ribbons have not yet been created. The flower-shaped objects (not five-petalled!) are usually seen embedded in f.c.c. aluminium (Boettinger, 1984) and are sometimes accompanied (Boettinger, 1984) by other Al-Mn phases. Each of the latter phases has well-defined physical boundaries. Since the flower-shaped specimens which exhibit icosahedral point-group symmetry are accompanied by other phases, it is difficult to isolate the object of interest. Electron diffraction is, among the possible diffraction techniques, a very useful probe because the size of the beam is comparable to the size of the crystal, and the stray f.c.c. aluminium spots can easily be isolated.

In the analysis of the electron diffraction patterns (Kuriyama, Long & Bendersky, 1985), the view that we adopted was that the specimen can be described as an imperfect real crystal in which lattice translations do not necessarily hold (Kuriyama & Miyakawa, 1969; Kuriyama, 1970, 1975). This starting point should not bias the analysis since no particular symmetry or lattice is assumed. It will be demonstrated below that the atomic positions for the icosahedral structure can be given based on a reference crystal lattice. In this model, three-dimensional modulations may appear as atomic correlations, rather than as weaker modulations in one or two dimensions (Dehlinger, 1928; Fujiwara, 1957; de Fontaine, 1966), as have beeen extensively studied in the past. While this work was under way, we learned of two papers (Bak, 1985; Nelson & Sachdev, 1985) that suggest that the icosahedral structures belong to the larger class of incommensurate modulated structures, where the focus of those works was Landau-Ginsberg theory.

2. Analysis in momentum space

With the Born (kinematical scattering) approximation, the scattering amplitude for a system lacking lattice translational invariance is given by

$$S(\mathbf{k}) = V^{-1} \int \mathrm{d}^3\mathbf{r}\,\varphi(\mathbf{r}) \exp\left[-i(\mathbf{H}+\sum_i n_i\mathbf{q}_i)\cdot\mathbf{r}\right] \times\left[(2\pi)^3\delta(\mathbf{k}-\mathbf{H}-\sum_i n_i\mathbf{q}_i)\right]. \quad (1)$$

V is the volume of the sample that is exposed to the incident beam; $\varphi(\mathbf{r})$ is either the electron charge density for X-rays, the Coulomb potential for electrons, or the nucleon potential in the case of neutrons.

H is the reciprocal-lattice vector for an arbitrary reference crystal lattice, and the $\mathbf{q}_i$'s describe the deviations from the reference reciprocal lattice (or the modulations). n_i takes the value of zero or positive or negative integers.

The scattering amplitude is the product of two factors: one is the scattering factor which includes electrons in the material, and the other is the geometrical structure factor which represents the three-dimensional construction of diffraction spots in reciprocal (momentum) space. The intersection of this construction with the Ewald sphere (a plane in the case of electron diffraction) gives the patterns of electron diffraction, or the X-ray patterns that would be obtained with a precession camera. The observed diffraction spots (**k**'s) can be sorted using the rule for momentum transfer: $\mathbf{k} = \mathbf{H} + \sum n_i \mathbf{q}_i$. These sets of **k**'s will be called 'reciprocal-lattice points'. The objective is to find the independent sets of $\mathbf{q}_i$'s and **H**, in other words, to find the nature of the incommensurate structure that leads to the observation of the special icosahedral symmetry.

Electron diffraction patterns were taken in five orientations as shown in Fig. 1. For convenience, three orthogonal axes are introduced, one of which is [001], perpendicular to the twofold pattern, and the other two ([100] and [010]) are parallel to the x axis and the y axis in Fig. 1. The twofold pattern was used to identify a reference reciprocal lattice in the (001) plane. Since lattice translational invariance does not necessarily hold, the choice of **H** is arbitrary. It has proven useful to select reasonably spaced spots within a limited area (Fig. 2). Since there is a periodic repetition of the positions of the diffraction spots, the measured modulations form a finite set. One may start with redundant sets since these can be reduced at the end to the smallest number of independent sets. An early check of the accuracy of the measured modulations and the assumed reference lattice is a comparison of the experimental pattern and a calculation of the reciprocal-lattice points in the (001) plane.

Next, the Ewald sphere (plane) is rotated about either [100] or [010] by the amount indicated in Fig. 1. The reciprocal-lattice points in the direction perpendicular to the rotation axis add partial information on the arrangements of the reciprocal-lattice points in the (100) and the (010) planes. In this manner, a three-dimensional reconstruction of the reciprocal-lattice points is complete. The calculated intersections of these reciprocal-lattice points with the Ewald sphere (plane) are shown in Fig. 3 next to the measured patterns for comparison. The agreement between the positions of observed diffraction spots and those in the calculated patterns is very good. This demonstrates that the modulations measured in the twofold pattern form a complete set in that the threefold, the fivefold and the apparent mirror patterns are completely indexed.

The next stage is to reduce the exhaustive sets of $\mathbf{q}_i$'s (we used 42) to the independent sets of $\mathbf{q}_i$'s, and also to determine whether the reference reciprocal lattice, $\mathbf{H} = h\mathbf{b}_1 + k\mathbf{b}_2 + l\mathbf{b}_3$, exists as an unmodulated structure. The results are:

1. there are two sets of six independent modulations $\{\mathbf{q}_i^{(1)}\}$ and $\{\mathbf{q}_i^{(2)}\}$ $(i = 1, \ldots, 6)$, as listed in Table 1, instead of the three independent vectors normally required to identify diffraction spots;

2. all six modulations in each set have the same magnitude $[|\mathbf{q}_i^{(1)}| = |\mathbf{q}_j^{(1)}|$ and $|\mathbf{q}_i^{(2)}| = |\mathbf{q}_j^{(2)}|]$, where the ratio of the magnitude in set (1) to that in set (2) is approximately four;

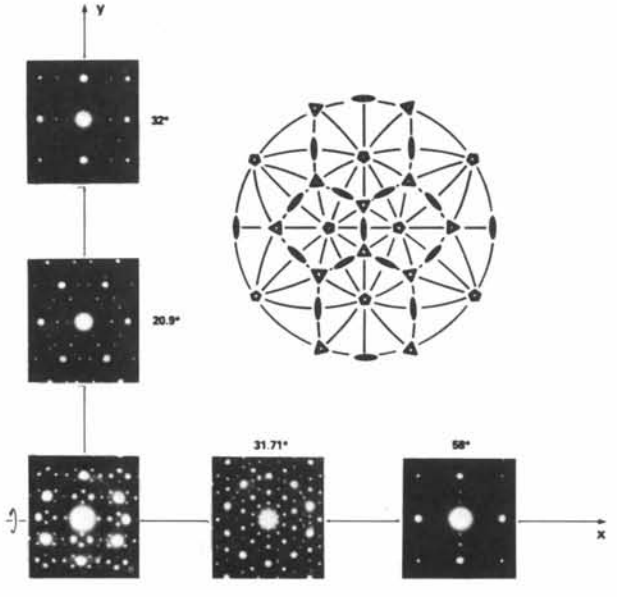

Fig. 1. A set of five electron diffraction patterns taken from rapidly cooled Al-14 at. % Mn. The inset shows the stereographic projection of axes in the icosahedral symmetry. A twofold pattern is at the origin of the x and y axes; angles indicate rotations about the respective axes.

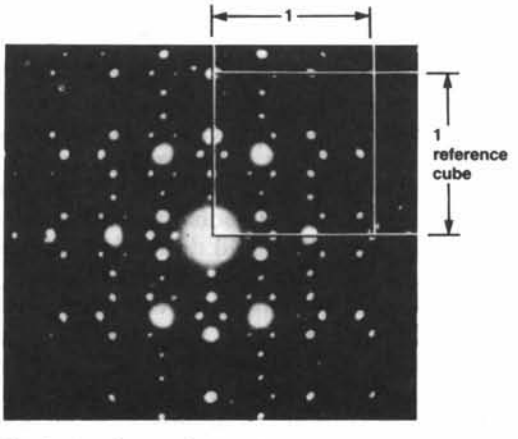

Fig. 2. A reference frame shown to a twofold pattern.

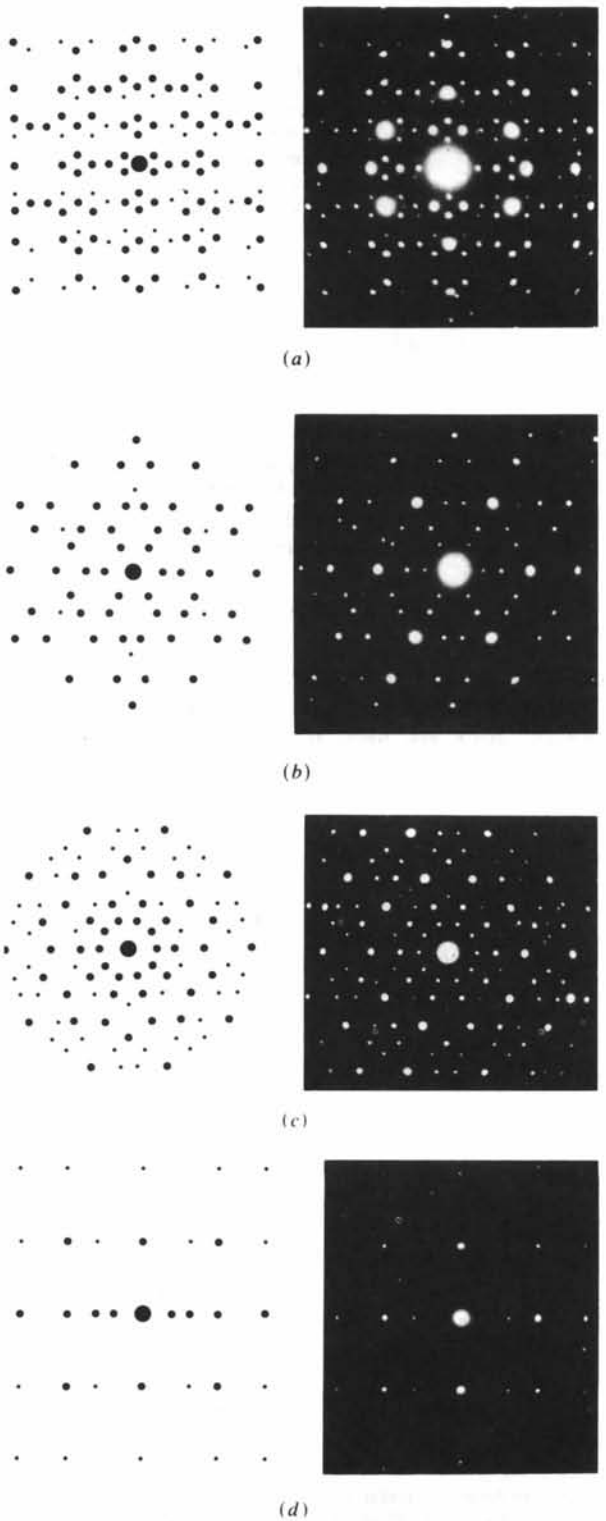

Fig. 3. Comparison of the observed patterns (right) and the calculated patterns (left). The reciprocal-lattice points are constructed from the oberved patterns using an arbitrary reference reciprocal lattice and the accompanying modulations. (*a*) Twofold pattern; (*b*) threefold pattern; (*c*) fivefold pattern; and (*d*) apparent mirror pattern. (The sizes of spots were selected for convenience, since it is premature to attempt an intensity calculation.)

Table 1. *Measured modulations*

These quantities were measured in cm; the value of λL (the electron diffraction camera constant) was $6{\cdot}77\times10^{-12}$ m^2.

$\mathbf{q}_1^{(1)} = (0{\cdot}64, 0{\cdot}40, 0{\cdot}00)$	$\mathbf{q}_1^{(2)} = (2{\cdot}65, 1{\cdot}65, 0{\cdot}00)$
$\mathbf{q}_2^{(1)} = (0{\cdot}40, 0{\cdot}00, 0{\cdot}64)$	$\mathbf{q}_2^{(2)} = (1{\cdot}65, 0{\cdot}00, 2{\cdot}65)$
$\mathbf{q}_3^{(1)} = (0{\cdot}00, 0{\cdot}64, 0{\cdot}40)$	$\mathbf{q}_3^{(2)} = (0{\cdot}00, 2{\cdot}65, 1{\cdot}65)$
$\mathbf{q}_4^{(1)} = (-0{\cdot}40, 0{\cdot}00, 0{\cdot}64)$	$\mathbf{q}_4^{(2)} = (-1{\cdot}65, 0{\cdot}00, 2{\cdot}65)$
$\mathbf{q}_5^{(1)} = (0{\cdot}00, 0{\cdot}64, -0{\cdot}40)$	$\mathbf{q}_5^{(2)} = (0{\cdot}00, 2{\cdot}65, -1{\cdot}65)$
$\mathbf{q}_6^{(1)} = (0{\cdot}64, -0{\cdot}40, 0{\cdot}00)$	$\mathbf{q}_6^{(2)} = (2{\cdot}65, -1{\cdot}65, 0{\cdot}00)$

3. the modulation directions of the two sets are identical, within experimental error, and each set has the two angles (63·4 and 116·6°) related to icosahedral symmetry; and

4. the reference reciprocal-lattice vectors are created by the sums of two $\mathbf{q}_i^{(1)}$ vectors. Another possible reference lattice is given by the differences of the same vector pairs. Thus, the original unmodulated structure (the underlying reference lattice) cannot be uniquely identified. In other words, the positions of the reference lattice points can be found in terms of the 'modulation vectors'. This result is astonishing within the framework of the normal concept of incommensurate crystals.

Using only the two sets of modulations derived above, the properties of the diffracted intensity can be explained phenomenologically using the scattering amplitude [in particular, the first factor in (1)], even before having information on the exact Al and Mn sites in the structure. If the electron charge density around the atoms is assumed to be spherically symmetric, the scattering factor yields the intensities obeying the icosahedral symmetry about the incident beam. Further, if the electron charge distribution is assumed to be slowly varying, the intensities for different orders n_i are given by the modulus square of the amplitude in the form

$$\left\{\sin\left[M_j\sum n_i(\mathbf{q}_i^{(j)}\cdot\boldsymbol{\varepsilon})\right]/M_j\sum n_i(\mathbf{q}_i^{(j)}\cdot\boldsymbol{\varepsilon})\right\}$$
$$\times\exp\left[-M_j\sum(n_i\mathbf{q}_i^{(j)}\cdot\boldsymbol{\varepsilon})\right],$$

where M_j is an appropriate length scale along the direction $\boldsymbol{\varepsilon}$. This behavior was shown by Levine & Steinhardt (1984) as derived from the one-dimensional case.

In electron diffraction, the Ewald sphere (plane) intersects many reciprocal-lattice points for a given beam geometry, and this results in the simultaneous excitation of Bragg conditions. The kinematical scattering approximation is then inadequate to explain properly the intensities in electron diffraction patterns. What would be required is the phase object approximation (Cowley, 1981), or the dynamical theory for many beams (Sturkey, 1957; Fujimoto, 1959; Niehrs, 1959; Kuriyama, 1970, 1975).

3. Structure in real space

3.1. *Atomic arrangement*

In the previous section, the momentum space data in the twofold electron diffraction pattern were analyzed to determine the two sets of six modulation vectors required for indexing the two-, three- and fivefold icosahedral patterns. It was shown that these modulations yield the angles and distance scale relevant to the icosahedral point group. They can also be used to gain insight into the three-dimensional arrangement of atoms for this special symmetry, as we will show in this section. For this purpose it will be useful to retain a cubic coordinate system, even though the original cubic reference lattice is no longer uniquely defined.

When the two sets of modulations, $\mathbf{q}_i^{(j)}$, are converted into modulation distances in real space, the magnitudes of $\mathbf{r}_i^{(1)}$ and $\mathbf{r}_i^{(2)}$ are found to be approximately* 4·34 and 1·05 Å respectively, where $\mathbf{r}_i^{(j)}$ is parallel to $\mathbf{q}_i^{(j)}$. Therefore, $\mathbf{r}_i^{(1)}$ is also parallel to $\mathbf{r}_i^{(2)}$. The direction cosines of the $\mathbf{r}_i$ are given in Table 2. It is noteworthy that, within experimental error, the following relation holds for the angle θ given in Table 2:

$$\sin\theta\cos\theta = \cos^2\theta - \sin^2\theta. \qquad (2)$$

The modulation distances $\mathbf{r}_i^{(1)}$ are assumed to correspond to the correlation distances between atomic scatterers. That is, the $\mathbf{r}_i^{(1)}$ set will be considered to represent some of the interatomic distances in the structure. It is not necessary that the nearest-neighbor distances are among the assumed correlations.

Since the vector sets are identical in direction, differing only in their magnitudes, only one set, the $\mathbf{r}_i^{(1)}$ set, will be considered here. The six vectors separate naturally into two sets of three where three have an included angle of 63·4°, and the other three have an included angle of 116·6°. To gain insight into the packing of atoms, one can use Friedel's law. This means that one cannot *a priori* determine whether the two sets of three vectors all points 'upwards' or if some of them point upwards and others downwards (Fig. 4*a*). Since these vectors are taken to represent some of the atomic correlations, some possible positions of the atoms within two rhombohedra are identified in relation to atom 0 as shown in Figs. 4(*b*) and (*c*). One of these rhombohedra has a pointed shape ($\alpha = 63.4°$) and the other has a flat shape ($\alpha = 116.6°$). These positions of atoms on the six rhombohedral faces provide a guide for maintaining fivefold symmetry when the two rhombohedra are used to fill

Table 2. *Direction cosines for the interatomic distances*

$|\mathbf{r}_i^{(1)}| = 4{\cdot}34$ Å; $|\mathbf{r}_i^{(2)}| = 1{\cdot}05$ Å and $\theta = 31.717°$. See footnote to §3.1.

$\mathbf{r}_1$	$(\cos\theta, \sin\theta, 0)$
$\mathbf{r}_2$	$(\sin\theta, 0, \cos\theta)$
$\mathbf{r}_3$	$(0, \cos\theta, \sin\theta)$
$\mathbf{r}_4$	$(-\sin\theta, 0, \cos\theta)$
$\mathbf{r}_5$	$(0, \cos\theta, -\sin\theta)$
$\mathbf{r}_6$	$(\cos\theta, -\sin\theta, 0)$

three-dimensional space. For example, the distances between atom 1 and atom 5_2 and between atom 3 and atom 5_2 are given by $|\mathbf{r}_1 - (\mathbf{r}_2 + \mathbf{r}_5)|$ and $|\mathbf{r}_3 - (\mathbf{r}_2 + \mathbf{r}_5)|$, respectively, and are found to be equal because of (2). These distances are also equal to $|\mathbf{r}_3 + \mathbf{r}_4 + \mathbf{r}_5|$, which is the distance between atom 1 and atom 3+4. Thus, one atomic site, say 5_2 in Fig. 4(*b*), on the face of a pointed rhombohedron becomes equivalent to a site on the tip (3+4) of the shortest body diagonal of a flat rhombohedron sharing atom 0.

3.2. *Model I: number density* 1-*to*-1

The atomic arrangement derived above guarantees icosahedral point-group symmetry within the volume of three-dimensional space when the two decorated rhombohedra are used to fill space with number density of one pointed to one flat rhombohedron.

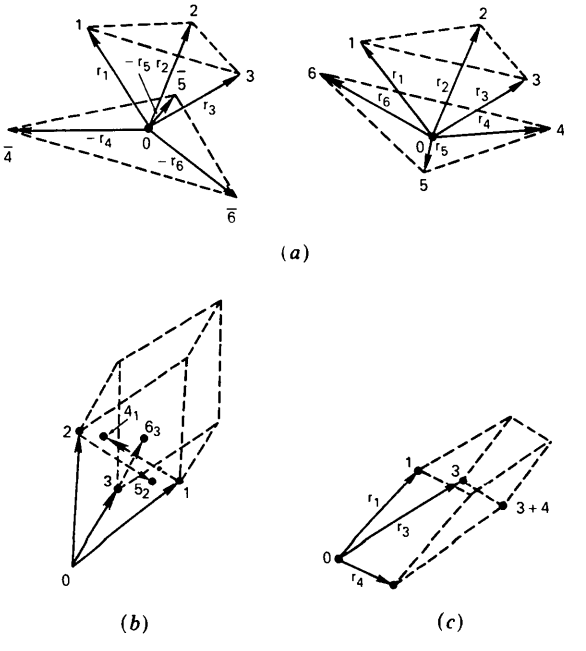

Fig. 4. (*a*) Atomic correlations. 0 is an atom at the origin. 1, 2 and 3 are atoms located distances $\mathbf{r}_1$, $\mathbf{r}_2$ and $\mathbf{r}_3$ from 0. 4, 5 and 6 are atoms located distances $\mathbf{r}_4$, $\mathbf{r}_5$ and $\mathbf{r}_6$ from 0. $\bar{4}$, $\bar{5}$ and $\bar{6}$ are atoms located distances $-\mathbf{r}_4$, $-\mathbf{r}_5$ and $-\mathbf{r}_6$ from 0. (*b*) Possible atomic positions in the pointed rhombohedron. 4_1 is located a distance $\mathbf{r}_4$ from atom 1. 5_2 is located a distance $\mathbf{r}_5$ from atom 2. 6_3 is located a distance $\mathbf{r}_6$ from atom 3. (*c*) Possible atomic positions in the flat rhombohedron. 3+4 is a possible atomic site. All other corners are shared.

* All lattice parameters and interatomic distances depend on the size of the vectors **q**. Since the experimental error is quite large (~10%), the distances quoted are to be understood as relative and an adjustment of one distance (due to future more accurate experiments) will require the concurrent adjustment of all the distances.

Using the angles between the rhombohedra given by the data, the filling ('tiling') of real space is accomplished when the faces of the pointed (63·4°) rhombohedra touch only the faces of the flat (116·6°) ones and *vice versa*. With this tiling, there is no ambiguity concerning the positions of the atomic sites on rhombohedral faces. The resulting structure has four true threefold axes 70·53° apart, along which the longest and shortest body diagonals of the pointed and the flat rhombohedra respectively are aligned. These directions are ⟨111⟩ axes, or a ⟨111⟩ axis and three of the other threefold axes in the icosahedral symmetry.

All of the properties of the icosahedral point group are accommodated in this structure. The fivefold, the threefold and the twofold axes are continuous through space, although the fivefold (and some of the threefold) axes are 'local'. An illustration of this is given in Fig. 5. For this figure, 32 flat and 32 pointed (decorated) rhombohedra were used. A cut perpendicular to a fivefold face is shown in Figs. 5(*a*) and (*b*), with the rhombohedral edges shown in Fig. 5(*a*) for reference. Cuts perpendicular to a true threefold (Figs. 5*c* and *d*), twofold (*e* and *f*), and a local threefold (*g* and *h*) axis are also given. The atomic motif created using decorated rhombohedra conforms to icosahedral symmetry, but we note that the simple geometrical three-dimensional packing of *undecorated* rhombohedra does not conform to icosahedral symmetry within the volume. This is similarly true for the rhombic triacontahedron, despite superficial appearances to the contrary.

The pattern of atomic sites shown in Fig. 5 was derived from a set of displaced rotations about four axes 70·53° apart. Another way of looking at this construction is to consider a group of four flat and four pointed (decorated) rhombohedra appropriately aligned (Fig. 6). These can be spatially translated along three basis vectors: $\mathbf{a}_1=\mathbf{r}_1+\mathbf{r}_5$, $\mathbf{a}_2=\mathbf{r}_2+\mathbf{r}_6$ and $\mathbf{a}_3=\mathbf{r}_3+\mathbf{r}_4$. Such translations restore the original arrangement of rhombohedra and continue the pattern of atomic sites. Using (2), the $\mathbf{a}_i$'s are shown to be mutually orthogonal and equal in magnitude to $2r\cos\theta$. From this point of view, the six $\mathbf{r}_i^{(1)}$'s represent a new crystal lattice with three independent basis vectors $\mathbf{a}_i$ given above.

The unit cell for this lattice is constructed of four flat and four pointed rhombohedra as mentioned above. It is a cubic-like structure that could be called 'icosahedral cubic' because the properties of the icosahedral point group are accommodated as shown in Fig. 5. Therefore, the same construction of Fig. 5

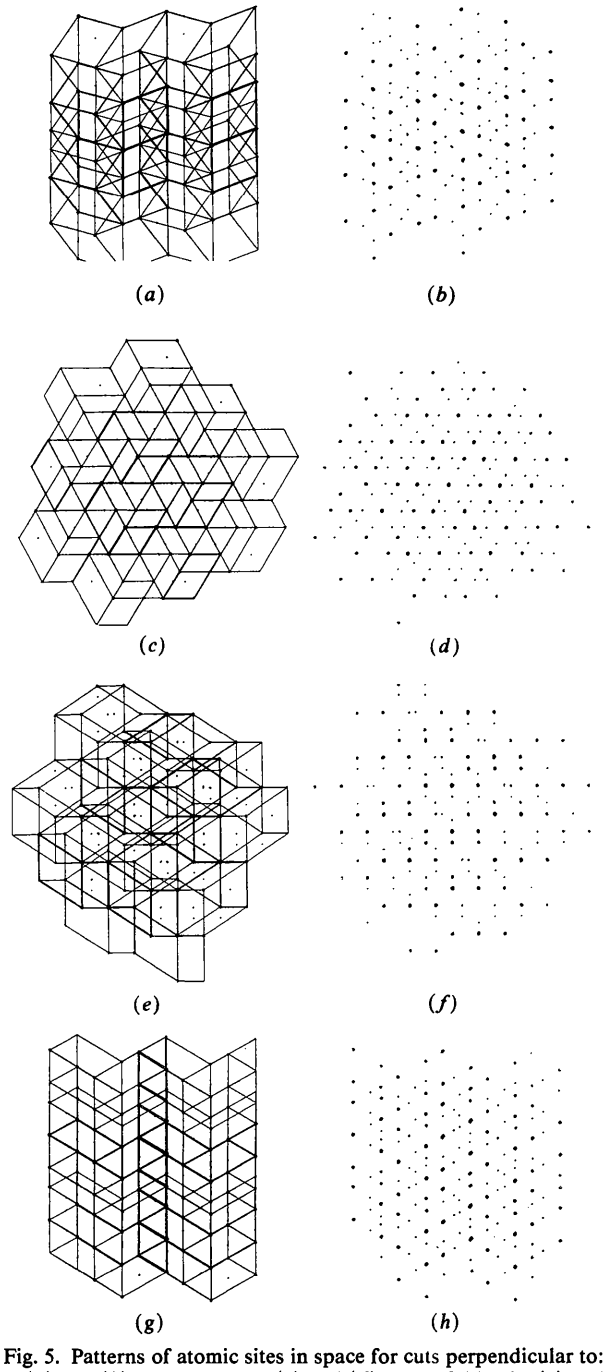

Fig. 5. Patterns of atomic sites in space for cuts perpendicular to: (*a*) and (*b*) a fivefold axis; (*c*) and (*d*) a threefold axis; (*e*) and (*f*) a twofold axis; (*g*) and (*h*) a local threefold axis.

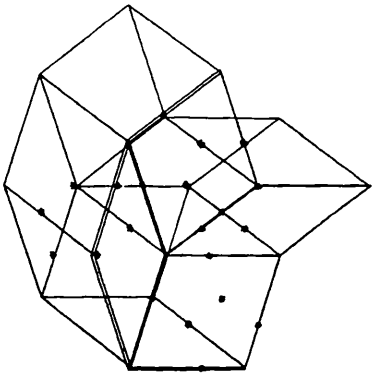

Fig. 6. Unit cell for model I. The cell is shown aligned perpendicular to a fivefold axis.

is realized using eight unit cells of Fig. 6 stacked $2\times2\times2$. The lattice parameter of the icosahedral cubic cell is $a=7{\cdot}38$ Å* and it contains sites for 32 atoms. Eight atomic sites are on the vertices and 24 sites are on the faces of the rhombohedra. The position of an atom is given by

$$\mathbf{R}(\mathsf{n})=\sum n_i\mathbf{r}_i, \tag{3}$$

where n indicates a set of integers $\{n_i\}$. (This expression is valid throughout the crystal.) Along a fivefold axis, say $\mathbf{r}_1$, an atom can be located at a site given by

$$d_n=[\mathbf{r}_1\,.\,\mathbf{R}(\mathsf{n})]/r=d\left[\sum_{2,3}n_i+\sum_{4,5,6}n_i\right]+n_1r,$$

where d is a spacing given by $(\mathbf{r}_1\,.\,\mathbf{r}_i)/r$ and $r=|\mathbf{r}_1|$. The spacing d is the distance between the 0-atom plane and the adjacent plane of atoms above or below. This value is about 45% of r. The plane above and the plane below together form a puckered layer of atoms in this structure. If we suppose that r is approximately twice the size of d, then the puckered layer spacing is

$$\begin{aligned}d_n&=\left(\sum_{2,3}n_i+\sum_{4,5,6}n_i+2n\right)d\\&=\text{integer}\times d.\end{aligned}$$

The result is a structure that is three-dimensionally layered with layering along each of the fivefold directions.

With regard to the threefold directions, the elevation of an atom along the ⟨111⟩ direction is given by

$$\begin{aligned}\mathbf{e}\,.\,\mathbf{R}(\mathsf{n})&=r\left\{(\mathbf{e}\,.\,\mathbf{r}_1)\sum_{1,2,3}n_i+(\mathbf{e}\,.\,\mathbf{r}_4)\sum_{4,5,6}n_i\right\}\\&=r(\mathbf{e}\,.\,\mathbf{r}_4)\left\{c\sum_{1,2,3}n_i+\sum_{4,5,6}n_i\right\},\end{aligned}$$

where $\mathbf{e}$ is a unit vector along the ⟨111⟩ direction and c is the ratio of $(\mathbf{e}\,.\,\mathbf{r}_1)$ to $(\mathbf{e}\,.\,\mathbf{r}_4)$. From the measured values of $\mathbf{r}_i^{(1)}$, c is found to be equal to $2\tau+1$ or τ^3. That is, the shortest body diagonal of the flat rhombohedron is 4·2 times shorter than the longest body diagonal of the pointed rhombohedron. The numerical relationship between these body diagonals is probably related to the second set of modulations $\mathbf{q}_i^{(2)}$ as we will show below. The ratio of magnitudes of $\mathbf{r}_1^{(1)}$ to $\mathbf{r}_i^{(2)}$ is approximately 4·1–4·2, which agrees well with the value of c given above.

In retrospect, the assignment of the $\mathbf{r}_i^{(1)}$'s to correlation distances rather than to ordinary modulations was justified. It permits the decoration of rhombohedra in this model by imagining 'interpenetrating' rather than merely 'space-filling' rhombohedra. With space-filling rhombohedra, an atom is usually only assumed to exist at each vertex. Mathematically, the imaginary interpenetrating rhombohedral construction leads to a derivation of possible atomic sites with physically plausible coordinations of nine to ten, while maintaining icosahedral ordering. Relative distances derived from this model are given in Table 3.

Table 3. *Nearest atomic distances* (Å)

See footnote to §3.1.

$MnAl_6$	
Average Mn-Al distance	2·56
Average Al-Al distance	2·78
Shortest Mn-Al distance	2·44
Shortest Mn-Mn distance	4·50
Next Mn-Mn distance	4·99
Icosahedral Mn-Al	
Atom 1 to atom (3+4)	2·44
Atom 5_2 to atom 3 or 1	2·44
Rhombohedron edge	4·34
Atom 1 to atom 2	4·56
Atom 5_2 to atom (1+3)	4·80

3.3. *Diffraction properties of the model I lattice*

Although the unit cell derived in the previous section conforms to the icosahedral point-group symmetry, one cannot expect a 'cubic' cell to produce the observed icosahedral point-symmetry diffraction patterns. The icosahedral cubic cell can be considered at this stage to be a relevant 'reference lattice' for this special structure. Normally, one adds 'modulations' to a reference lattice to explain extraordinary diffraction patterns. It is already clear that the character of these modulations must be different from what is normally seen in modulated structures because *all* the spots are found by $\sum n_i\mathbf{q}_i$ and, for any arbitrary reference lattice **H**, the diffraction spots referred to as **H** are also found as a sum of $\mathbf{q}_i$'s. In this paper we only mention possible ways of incorporating 'modulations' into model I.

One way to proceed is to recall that the diffraction spots require six indices rather than the usual three for the purpose of indexing. Then, the three orthogonal vectors that describe the unit-cell edges are seen as only a partial representation of the degrees of freedom. The three remaining degrees of freedom can be found from a sublattice such as: $\mathbf{a}_1^+=\mathbf{r}_1-\mathbf{r}_6$, $\mathbf{a}_2^+=\mathbf{r}_2-\mathbf{r}_4$ and $\mathbf{a}_3^+=\mathbf{r}_3-\mathbf{r}_5$. These vectors are mutually orthogonal and equal in magnitude to $2r\sin\theta$ or 4·56 Å.* Looking at the atomic sites inside a unit cell, one finds sites related to such sublattices. Two sublattices aligned along each ⟨111⟩ direction can be found. A coherent arrangement of the sublattices and the reference lattice may require some local adjustments to avoid unphysical atomic distances. These adjustments, if applied, would have to conform to the

* See footnote to §3.1.

* See footnote to §3.1.

second set of modulations, $\mathbf{q}_i^{(2)}$, that were observed in the diffraction patterns.

The coherent coexistence of the reference lattice and sublattices would appear in diffraction as two or more crystals in one. The coherence could easily be achieved in this particular case because the lattice and sublattices share many of the same atomic sites. (This coherent coexistence of two lattices is not a microdomain model because neither lattice dominates an extended local area.) Let the reciprocal lattice of $\{\mathbf{a}_j\}$ and $\{\mathbf{a}_j^+\}$ be $\{\mathbf{b}_j\}$ and $\{\mathbf{b}_j^+\}$, respectively. Then the momentum transfer $\Delta\mathbf{k} = h\mathbf{b}_1 + k\mathbf{b}_2 + l\mathbf{b}_3 + h'\mathbf{b}_1^+ + k'\mathbf{b}_2^+ + l'\mathbf{b}_3^+$, which is equal to $(h+h')\mathbf{q}_1 + (k+k')\mathbf{q}_2 + (l+l')\mathbf{q}_3 + (l-k')\mathbf{q}_4 + (h-l')\mathbf{q}_5 + (k-h')\mathbf{q}_6$. (The $\mathbf{q}_i$'s are the reciprocal vectors of the r_i's as above.) Then, all six of the $\mathbf{q}_i$ vectors participate in the scattering, rather than as $\mathbf{b}_j$ or $\mathbf{b}_j^+$ alone.

As described above, the coexisting lattice model requires local adjustments consistent with an additional set of modulations: $\mathbf{q}_i^{(2)}$. Since the set $\mathbf{q}_i^{(2)}$ was observed experimentally, this set of modulations could have been used from the outset as physical modulations in the material. Then, since the magnitude of the $\mathbf{q}_i^{(2)}$'s are all almost equal to $2\tau + 1 = \tau^3$, the momentum transfer is again given by the sums of the six $\mathbf{q}_i$ vectors. In this case, our perception of the nature of this set of modulations is different. The existence of modulation vectors with the magnitude τ^3 leads to the lattice sites associated with $\{\mathbf{a}_i^+\}$, but it may be possible to bypass the concept of sublattices. In either case, accepting the $\mathbf{q}_i^{(2)}$ as a guide to modulations on a reference lattice requires a generalization of the usual concept of modulated crystals.

The appearance of the diffraction patterns revealing point-group symmetry inconsistent with lattice translations can be understood then either by a model involving coexisting reference lattice and sublattices, or by the acceptance of the observed modulations as a physical phenomenon. Both approaches lead to the recognition of $\{\mathbf{a}_i^+\}$, independent of whether these three vectors are regarded as forming sublattice(s) or not.

The relationship between the reference lattice derived from the $\mathbf{q}_i^{(1)}$ and the modulations introduced *via* the $\mathbf{q}_i^{(2)}$, and the implications on ordering and occupancy of atomic sites are explored in the following paper (Kuriyama & Long, 1986).

3.4. *Model II*: *number density* 1-*to*-τ

Using a similar atomic arrangement to that in model I, it is possible to create another reference-periodic model, where now the face of a pointed rhombohedron may touch the face of another pointed rhombohedron, and the same is true for the flat rhombohedra. In this case, there will be some ambiguity regarding the sites on the faces of rhombohedra. The number density of the space-filling object in this case is nearly in the ratio of one flat to τ pointed rhombohedra. The unit cell is built up of rhombic triacontahedra, one of which is centered at each of the corners of a tetragonal unit. On the single short side, two triacontahedra touch on a twofold face. On the two longer sides, interpenetrating triacontahedra are seen. The ratio of a/c is τ. This unit cell is a faulted version of the nonperiodic three-dimensional tiling where one would have 89 rhombohedra in a model of this size: 34 flat and 55 pointed. Instead, there are 32 flat and 52 pointed. The two missing flat rhombohedra are shared between three triacontahedra (*i.e.* along a threefold direction), and the three missing pointed rhombohedra are similarly removed to create modulations along the threefold directions, to conform with the $\mathbf{q}_i^{(2)}$.

The lattice parameters are $a = 19{\cdot}33$ and $c = 11{\cdot}95$ Å,* making model II much larger and more complex than model I. Presumably, larger and larger cells could be created, with increasingly fewer faults relative to a perfect aperiodic tiling. This model also involves an intrinsic anisotropy.

4. Discussion

Both model I and model II require that the atoms in the structure are quite close together. The atoms within the rhombohedra have atomic distances* as listed in Table 3. These are to be compared to the known distances in the $MnAl_6$ structure (Nicol, 1953), which has a similar atomic fraction of Mn to the alloy structure under investigation.

In $MnAl_6$, some of the Mn and Al atoms are known to be unusually close to each other.† In the proposed models, the closest of the derived distances is the same as the closest of the distances in the known crystalline structure, while the rest of the derived distances are generally smaller than the average distances in that structure. If all the sites of model I were occupied, then the structure would be approximately 19% more dense than orthorhombic $MnAl_6$.

It can be seen from both of the models that the known layering of $MnAl_6$ is extended to layering in all six of the fivefold directions of the icosahedral symmetry. Models I and II are similar to one another in that a similar atomic packing is used for both in order to satisfy the requirements of the icosahedral point-group symmetry within the volume, and that the overall building blocks are the same flat and pointed rhombohedra. There the similarity ends, because model I is isotropic and has a simple unit

* See footnote to §3.1.

† Recent EXAFS results (E. A. Stern *et al.*, preprint) rule out the shortest Al–Mn distance in icosahedral phase Al–Mn alloys. With their value for this distance, the distances in this model are scaled up by 5%. This changes the density of the model to 6% more dense than $MnAl_6$ if all sites are filled.

cell with four flat and four pointed rhombohedra, and model II has a complicated unit cell involving 32 flat and 52 pointed rhombohedra, plus rules for accommodating modulations. Model II bears an obvious resemblance to the aperiodic structures attempted by others (*e.g.* Levine & Steinhardt, 1984). In view of the success of model I in leading to the derivation of additional periodicities through sublattices, and in explaining the possibility of observing icosahedral diffraction patterns, it is preferred for its physical plausibility over either the model II unit cell or the undecorated aperiodic structures.

In conclusion, the electron diffraction patterns taken from icosahedral phase Al-Mn can be understood in terms of an icosahedral cubic reference lattice derived from six modulation vectors $\mathbf{q}_i^{(1)}$ plus six collinear modulations $\mathbf{q}_i^{(2)}$. The appearance of the six $\mathbf{r}_i$'s may be taken together with theoretical results of Bak (1985). However, if the model derived in this work is to be understood within the context of ordinary incommensurate modulated crystals, the theory would have to be generalized to include structures for which the observed point symmetry is already realized in the unit cell of the reference lattice. Naturally, the pattern of atomic sites in this derived unit cell of the reference lattice is excluded from the 230 space groups because it conforms to icosahedral point symmetry.

In retrospect, once the experimental data required six independent vectors for indexing the diffraction pattern and for the construction of an atomic motif, the appearance of more than one three-dimensional periodicity was inevitable. In the following paper (Kuriyama & Long, 1986) the full mathematical structures of the **a** cell and the $\mathbf{a}^+$ sublattices are given. It is also shown how they are accommodated into a structure consistent with both sets of modulation vectors. In that work the full structure factor in terms of atomic positions is derived.

The authors gratefully acknowledge assistance with the experiment by L. Bendersky. We are also indebted to H. Fowler for his calculations in the preparation of Figs. 5 and 6, and to R. Roth for useful discussions.

References

BAK, P. (1985). *Phys. Rev. Lett.* **54**, 1517-1519.

BOETTINGER, W. J. (1984). Private communication.

COWLEY, J. W. (1981). *Diffraction Physics*, 2nd ed. Amsterdam: North Holland.

DEHLINGER, U. (1928). *Kristallografiya*, **65**, 615-631.

FONTAINE, D. DE (1966). *Local Atomic Arrangements Studied by X-ray Diffraction*, edited by J. B. COHEN & J. E. HILLIARD, pp. 51-94. New York: Gordon & Breach.

FUJIMOTO, F. (1959). *J. Phys. Soc. Jpn*, **14**, 1558-1568.

FUJIWARA, K. (1957). *J. Phys. Soc. Jpn*, **12**, 7-13.

HOGGATT, V. E. (1969). *Fibonacci and Lucas Numbers*. Boston: Houghton Mifflin.

KITTEL, C. (1976). *Introductioin to Solid State Physics*, 5th ed., p. 9. New York: John Wiley.

KRAMER, P. & NERI, R. (1984). *Acta Cryst.* A**40**, 580-587.

KURIYAMA, M. (1970). *Acta Cryst.* A**26**, 56-59.

KURIYAMA, M. (1975). *Acta Cryst.* A**31**, 774-779.

KURIYAMA, M. & LONG, G. G. (1986). *Acta Cryst.* A**42**, 164-172.

KURIYAMA, M., LONG, G. G. & BENDERSKY, L. (1985). *Phys. Rev. Lett.* **55**, 849-851.

KURIYAMA, M. & MIYAKAWA, T. (1969). *J. Appl. Phys.* **40**, 1697-1702.

LAUE, M. VON (1912). *Proc. Bav. Acad. Sci.* pp. 303-312, 363-372.

LEVINE, D. & STEINHARDT, P. J. (1984). *Phys. Rev. Lett.* **53**, 2477-2480.

MACKAY, A. L. (1981). *Sov. Phys. Crystallogr.* **26**, 517-522.

MACKAY, A. L. (1982). *Physica (Utrecht)*, **114**A, 609-613.

NELSON, D. R. & SACHDEV, S. (1985). *Phys. Rev. B*, **32**, 689-695.

NICOL, A. D. I. (1953). *Acta Cryst.* **6**, 285-293.

NIEHRS, H. (1959). *Z. Naturforsch. Teil A*, **14**, 504-511.

PENROSE, R. (1974). *J. Inst. Math. Its Appl.* **10**, 266-271.

SHECHTMAN, D., BLECH, I., GRATIAS, D. & CAHN, J. W. (1984). *Phys. Rev. Lett.* **53**, 1951-1953. [See also *Phys. Today*, (1985), **38**, 17-19.]

STURKEY, L. (1957). *Acta Cryst.* **10**, 858.

Acta Cryst. (1986). A**42**, 164-172

Single-Crystal Structure of Rapidly Cooled Alloys with Icosahedral Symmetry. II. Theoretical Analysis – Internal Modulations

BY MASAO KURIYAMA AND GABRIELLE GIBBS LONG

Institute for Materials Science and Engineering, National Bureau of Standards, Gaithersburg, MD 20899, *USA*

(*Received* 14 *August* 1985; *accepted* 4 *November* 1985)

Abstract

The icosahedral cubic cell, derived in the first of this set of two papers, is further developed. Rules for the occupancy of atomic sites are derived based on periodic modulations over the reference lattice. The form of the derived structure, which involves partial Fibonacci sequence stacking, suggests that the true structure is the limit of a superposition of successively larger periodic sequences. The structure factor for the limiting (nonperiodic) structure is derived and some physical insights into the application of almost periodic functions to icosahedral phase Al-Mn are given.